Available online at www.sciencedirect.com
SCIENCE DIRECT®
Journal of Crystal Growth 272 (2004) 739–747
JOURNAL OF CRYSTAL GROWTH
www.elsevier.com/locate/jcrysgro

Specific structural and compositional properties of (GaIn)(NAs) and their influence on optoelectronic device performance

Kerstin Volz*, Torsten Torunski, Bernardette Kunert, Oleg Rubel, Siegfried Nau, Stefan Reinhard, Wolfgang Stolz

Central Technology Laboratory, Material Sciences Center, Philipps University of Marburg, Hans-Meerwein Strasse, D-35032 Marburg, Germany

Abstract

We have grown (GaIn)(NAs) lattice-matched bulk as well as compressively strained multi-quantum-well structures by metal-organic vapour-phase epitaxy (MOVPE) suitable for either solar cell or laser applications, respectively. By applying a specific novel TEM dark-field technique columnar strain fields, which are possibly caused by chain-like N ordering in the samples, have been detected. Valence force field calculations show that indeed these chains are energetically stable in Ga(NAs). This chain-like ordering can be dissolved in (GaIn)(NAs), however, upon appropriate annealing, as verified experimentally. On the other hand we find that device performance especially of lasers is limited by carbon impurities in the active (GaIn)(NAs) region of the lasers. The strong affinity of N–C results in an enhanced incorporation of C if the N content in the material is increased. The paper also shows the sources of C incorporation in (GaIn)(NAs) MOVPE growth and how its incorporation can possibly be avoided.

PACS: 61.72.−y; 71.55.Eq; 68.37.Lp; 81.05.Ea; 81.15.Gh

Keywords: A1. Defects; A3. Metalorganic vapor phase epitaxy; B2. Semiconducting III/V materials; B3. Laser diodes; B3. Solar cells

1. Introduction

The novel, metastable compound semiconductor system (GaIn)(NAs) on GaAs introduced by Kondow et al. [1] is gaining increasing interest in recent years as it exhibits interesting electronic properties, such as the theoretically predicted [2,3]

*Corresponding author. Tel.: +49-6421-28-25694; fax: +49-6421-28-28935.
E-mail address: kerstin.volz@physik.uni-marburg.de (K. Volz).

0022-0248/$ - see front matter © 2004 Elsevier B.V. All rights reserved.
doi:10.1016/j.jcrysgro.2004.09.012

extreme band gap bowing. The excellent high-temperature characteristics make this material system very promising for long wavelength (1.3–1.55 μm) laser diodes for optical fibre communications. Apart from these laser applications, potential application of (GaIn)(NAs) in high-efficiency multi-junction solar cells are discussed [4]. (GaIn)(NAs) would be an optimal candidate as 1 eV solar cell material in multi-junction solar cell concepts, as it can be grown lattice matched to GaAs or Ge substrate. Up to now, the short minority carrier diffusion lengths, mainly of the electrons in the p-type regions, which are even shorter than the depletion widths in the devices, limit the performance of such cells [5–7]. Minority carrier diffusion lengths as low as 10–20 nm have been observed. This results in low short-circuit currents and low quantum efficiencies of the devices. It is crucial to determine whether these short diffusion lengths are due to extrinsic, growth-related defects or are an intrinsic property of this material system.

Lasers in this material system mostly suffer—irrespective of the growth technique metal-organic vapour-phase epitaxy (MOVPE) or MBE—from threshold current densities, which increase with increasing emission wavelengths towards 1.3 μm and beyond [8–10].

The present paper presents specific intrinsic structural and compositional properties of the metastable quaternary material, such as chain-like N ordering in growth direction and an enhanced C incorporation in the material with increasing N content. In addition this study discusses up to which extent optimised growth and annealing conditions can be found to circumvent these properties of the material and hence improve device performance.

2. Experimental procedure

All (GaIn)(NAs) and Ga(NAs) bulk or multi-quantum-well samples used for this study have been grown on (0 0 1) GaAs substrates in a commercially available horizontal reactor system (AIX200) by MOVPE using hydrogen carrier gas at a low reactor pressure of 50 mbar. As the material system under investigation is metastable, low substrate temperatures have to be chosen in order to achieve significant N incorporation. Substrate temperatures are usually fixed at 525 °C, if quantum-well samples are grown and to slightly higher temperatures (550 °C) if bulk material for solar cell application has been grown in order to compensate for the reduced diffusion possibility at the higher growth rate (1 μm/h) used for the bulk material. The substrate temperatures are calibrated to the Al/Si eutectic formation occurring at 577 °C. As a consequence of the low growth temperatures, MO sources efficiently decomposing at lower temperatures have to be used. We used the alternative group-V sources tertiarybutylarsine (TBAs) and the unsymmetric dimethylhydrazine (UDMHy). For certain growth experiments concerning the C incorporation into the quaternary (GaIn)(NAs) also tertiarybutyl hydrazine (TBHy) has been used as alterative N-precursor. For these studies, the substrate temperature has also been lowered to values between 350 and 500 °C, where we still find N incorporation from both N sources. As group III sources, we used triethylgallium (TEGa) and trimethylindium (TMIn). Our standard solar cell material shows both, lattice matching to GaAs and an 1 eV band gap at a composition of 8% In and 2.8% N [11]. We have applied annealing steps consisting of a 5 min TBAs stabilized anneal at 700 °C and a subsequent unstabilised annealing step at 625 °C for 25 min. Edge emitting (GaIn)(NAs) and (GaIn)As lasers have been grown over a wide range of parameters, varying the In composition, V/V and V/III ratios in the material and hence also the nitrogen content. These laser structures have been realized in a three-step epitaxy process using two MOVPE machines, which are connected to one another via a N_2 glove box. Samples have been transferred from one machine to the another after the first (AlGa)As cladding layer growth with a growth interruption in the SCH region for the growth of the N-containing material and than back to the first machine to grow the top cladding and contact. We found that the separation of N- and Al-containing material in the two machines is an important step towards achieving good laser performance. The broad area edge-emitting lasers were cleaved into bars of an area of $(100 \times 800)\,\mu m^2$

and were measured after front- and back-side contacting with no AR coating applied under pulsed excitation with a duty cycle of 200 ns/100 μs.

Those samples with a variety of In/N compositions adjusted under different growth conditions have also been utilised to quantitatively determine the C content in the quaternary material by secondary ion-mass spectrometry (SIMS). A carbon-implanted (GaIn)(NAs) sample was used as SIMS calibration standard and if C contents of thin QWs were extracted, special attention was paid to always compare samples with identical QW thickness. The integral In and N composition has been determined by HR X-ray diffraction (HRXRD) and dynamical simulation to the experimental patterns. Transmission electron microscopy (TEM) at an acceleration voltage of 300 kV with a special dark-field technique [12] was used to image strain fields in (GaIn)(NAs). To explain the observed strain contrast in the samples, we calculated the strain energy of the crystal for different N–N as well as N–In arrangements in the framework of the valence force field (VFF) model [13,14]. The input supercell contained 6346 atoms.

3. Results and discussion

The present paper is divided into two parts. The first one explains an intrinsic structural property of the quaternary metastable material, namely the formation of N chain-like ordering upon growth, its possible influence on material properties and possibilities to dissolve that ordering. In the second part we concentrate on carbon incorporation in N-containing material and show that there is a clear correlation between the C content in the active region of a laser and its threshold current density. The reminder of the paper will identify one of the sources of C in MOVPE growth and find growth conditions to minimize C incorporation and hence to optimise laser characteristics.

3.1. N ordering in (GaIn)(NAs)

A TEM (202) dark-field micrograph of an as-grown 500 nm thick $(Ga_{0.92}In_{0.08})(N_{0.028}As_{0.972})$ bulk film taken under strain sensitive imaging conditions is shown in Fig. 1(a). This material is the basis for our solar cell structures grown. Large columnar strain fields are clearly observed in the TEM DF micrograph. From previous investigations we know that the In is dispersed homogeneously throughout this complete film. Hence, In fluctuations cannot be the source of the large strain field fluctuations we observe in this

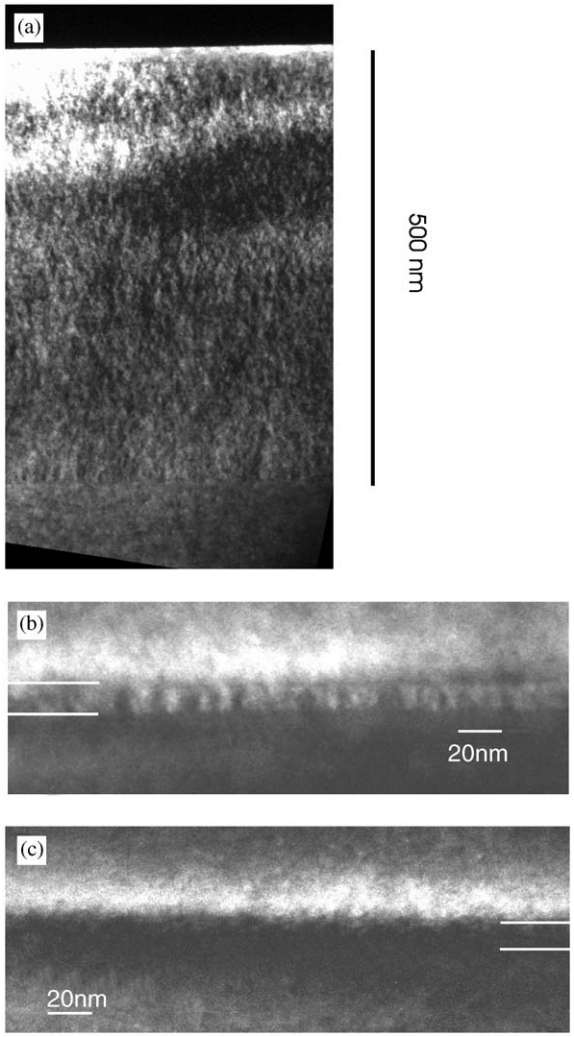

Fig. 1. Cross-sectional TEM (2 0 2) dark-field micrographs of a (GaIn)(Nas) bulk film, lattice matched to GaAs for solar cell applications (a) and dark-field micrographs of a (GaIn)(NAs) quantum well, emitting at 1.3 μm, before (b) and after (c) annealing.

structure. The alternating bright and dark contrast perpendicular to the (GaIn)(NAs)/GaAs interface, which has a lateral dimension in the order of 10 nm and a height of several 10 nm, is found throughout the complete structure. As the In is dispersed homogeneously in this sample, the only source for the strong strain undulations in the material can be the nitrogen, which is capable of introducing large strains in the material due to the short Ga–N bond length. A higher magnification micrograph, taken under identical excitation conditions from a $(Ga_{0.7}In_{0.3})(N_{0.025}As_{0.975})$ quantum well, emitting at 1.3 μm, is depicted in Fig. 1(b). Due to the lower overall thickness of the quaternary material, the strain fields can be seen a lot clearer in this sample. There exist columnar strain fields, which again can be identified by the alternating bright/dark contrast perpendicular to the (GaIn)(NAs)/GaAs interface. Also in this sample the In distribution does not show any fluctuations and hence those strain fields originate from the nitrogen. Annealing this quantum-well sample has a tremendous influence on the strain distribution in the sample, as can be seen from Fig. 1(c), where the dark field micrograph of the same sample as Fig. 1(b), but annealed under specific conditions, is shown. After the chosen annealing procedure the columnar strain fields have disappeared completely.

As we identified the N to be the source of those strain fields, we performed VFF calculations of different next nearest-neighbour configurations of N in GaAs and (GaIn)As. For Ga(NAs) first principle calculations have been reported in the literature [15,16]. The values for the strain of the different N configurations of our VFF calculations are summarised in Table 1 and fit very well to the values reported in the literature so that we conclude that our VFF model agrees with the first principle calculations and, thus, can also be applied to calculate further configurations in In containing material. Strain fields, to the extent observed, cannot be explained by the lattice distortion of a single N-atom in GaAs. Therefore, we concentrated on different N–N next nearest-neighbour configurations and find that [0 1 1] oriented N pairs have an even higher strain energy than two separated N atoms in GaAs. Therefore this configuration should not be adopted from the crystal upon growth. In contrast , we find–in accordance with Ref. [15,16]—that N ordering in [0 0 1] reduces the strain energy of the crystal by 0.19 eV as compared to putting two isolated N atoms in GaAs. This strain energy is even further reduced, when longer [0 0 1] oriented N chains in GaAs are formed. We attribute the columnar strain fields, which have the tendency to extend in growth directions and which we find in as-grown Ga(NAs) as well as (GaIn)(NAs) samples of different composition to this chain-like ordering of N upon growth into the thermodynamically stable configuration on the surface.

Upon annealing, strain with respect to the GaAs substrate in the bulk layer plays a more important role and what we experimentally observe (Fig. 1c), is the dissolution of the strain fields. This can also be theoretically explained by VFF calculations if we look for the influence of In on the strain in the crystal. In Table 2 the strain and total energies of N surrounded by 0–4 In atoms are listed. The strain of one single N atom is reduced by a factor of almost four if it goes from a four Ga to a four In configuration. Also taking the bonding energy into account, which is—due to the weakness of the In–N bond–reduced for In containing material, if

Table 1
Strain energies (eV) from VFF calculations of different N–N substitutional configurations in GaAs

Configuration	ΔE_{strain}
N_{As}	0
N–N [0 1 1]	+0.48
N–N [0 0 1]	−0.19
N–N –N [0 0 1]	−0.40

Table 2
Strain and total energies (eV) from VFF calculations for different N–In configurations in GaAs, with increasing number of N–In bonds

Local configuration	E_{strain}	ΔE_{strain}	ΔE_{chem}	ΔE
N–3Ga 1In	1.44	−0.69	0.23	−0.46
N–2Ga 2In	1.00	−1.31	0.46	−0.85
N–1Ga 3In	0.64	−1.85	0.69	−1.16
N–0Ga 4 In	0.4	−2.27	0.92	−1.35

N is put into an In-rich environment, we still calculate a significant decrease in total energy when N moves to a more In rich environment. This is what is also experimentally observed: the dissolution of the N chains, which are the stable configuration on the growth surface towards the favoured In–N bonds in the bulk upon annealing. This energy difference is also the driving force for the annealing-induced blue shift of the emission wavelength that is observed in the quaternary material [17,18]. This blue shift can be explained by a change in the N nearest-neighbour configuration upon annealing, resulting in a crystal with a different band gap than the as-grown one [18]. Investigations with local mode spectroscopy [19] also support this model. Upon annealing, an increase of In–N bonds at the expense of Ga–N bonds is observed in these studies.

From the device point of view, we observe a significant improvement of our solar cell performance upon annealing. On one side this might be correlated with dissolving the N chains, as the strain fields observed in the experimental images (Fig. 1(a) and (b)) have a strikingly equal distance (10–20 nm) than what has been reported to be the surprisingly short minority carrier diffusion length in (GaIn)(NAs) [6]. How far these chains deteriorate transport properties, to what extent special annealing conditions can be found to dissolve all of the chains as well as in low In containing solar cell material as in laser material and gain better electrical properties or to what extent these structural features might also be responsible for the strong carrier localization [20] observed in N containing material will be further clarified in detailed future studies.

3.2. Carbon incorporation in (GaIn)(NAs) and its influence on laser properties

Threshold current densities measured from edge emitting (GaIn)(NAs) and (GaIn)As lasers in dependence on the emission wavelength are depicted in Fig. 2. What one clearly observes is a strong overall increase of the threshold with increasing wavelength. Similar behaviour is also observed in the literature, irrespective of the growth technique, MOVPE or MBE [8–10]. The

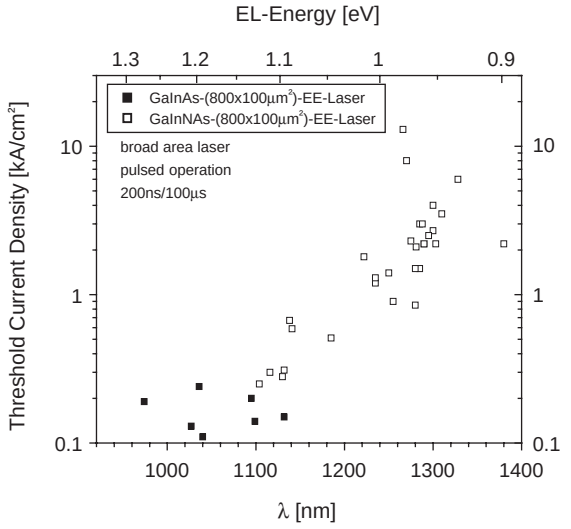

Fig. 2. Threshold current densities of (GaIn)((N)As)/GaAs broad area edge-emitting lasers in dependence of the emission wavelength.

data points more or less follow that trend and the scatter slightly increases. To yield all these data, samples have been grown with a variety of compositions and under completely different growth conditions. The remarkable fact is that the N-free (GaIn)As lasers show a significantly lower threshold current density compared to the N-containing (GaIn)(NAs) lasers. This might lead to the conclusion that N introduces a defect in the material, which is responsible for this significant increase in threshold current density (J_{th}). However, plotting J_{th} versus the N content in the samples instead of emission wavelength does not reduce the significant scatter in the data. Around 1.3 μm, we find a variation of J_{th} over one to two orders of magnitude. Also other possible dependencies of the threshold current density on In content, strain, V/V ratio etc. do not lead to a clear correlation.

Hence, a more detailed composition analysis by SIMS has been undertaken in order to clarify the source of this strong increase and the large variation of J_{th}. J_{th} in dependence on the calibrated C-content in the (GaIn)(NAs) and (GaIn)As quantum wells is shown in Fig. 3. One observes a direct correlation of J_{th} with the C content in the active material of the lasers. Hence,

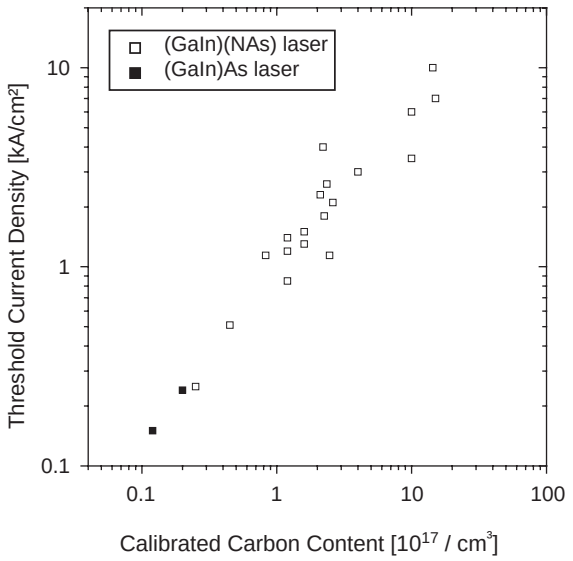

Fig. 3. Threshold current densities of (GaIn)((N)As)/GaAs broad area edge-emitting lasers in dependence of the carbon content in the quantum well.

we attribute the increase in J_{th} with emission wavelength to an increased C incorporation into the (GaIn)(NAs) active region of the devices. Carbon can act as a deep centre in (GaIn)(NAs) and hence traps carriers very efficiently. To what extent this C contamination also influences e.g. the temperature stability and lifetime of (GaIn)(NAs) VCSELs and VECSELs laser diodes will be clarified in future work.

The reminder of the paper will investigate the possible source of Carbon in MOVPE growth and find growth conditions to suppress its incorporation. The results of C–SIMS analysis of different samples with a variety of growth conditions in dependence of the N content in the samples are summarized in Fig. 4. The squares and circles denote conditions, where the partial pressure of the TBAs has been reduced or the partial pressure of the UDMHy has been increased under otherwise unchanged growth conditions. Both conditions result in an increased N incorporation as the V/V ratio is increased in both cases. For both cases we also find an increased C incorporation with increasing N content, i.e. reduction of TBAs and increase of UDMHy. As a consequence, we can exclude TBAs as the source of C incorporation, as C is reduced with increasing partial pressure of the arsenic MO source. To obtain the diamond data points, the In content in the samples has been varied under otherwise unchanged growth conditions, especially group V conditions. With increasing In concentration in the quaternary material one finds in MOVPE growth a reduction of the N incorporation, so that the data points for low N content correspond to the highest In content in the samples and hence to the highest TMIn partial pressure in the reactor during growth. From that, we can once again exclude the TMIn of being the source of C in the films, as C content drops with increasing In concentration, but increases with the N content in the samples. A similar behaviour is found for a reduction of the growth temperature results in an increase of the N and as we found also in the C content in the samples. These dependencies suggest that the C might be incorporated together with the N during growth—due to the strength of the C–N bond, which would not break again, once it formed. However, one opposite trend has been found, where the C content in the quaternary material can be reduced even if the N content is increasing. The upside down triangles depict conditions, under which the V/V ratio has been kept constant, but the partial pressures of both, UDMHy and TBAs, have been varied to yield different N contents in the samples. The dependence of the N content under constant V/V conditions on the UDMHy or TBAs partial pressure is rather complex [21], nevertheless, this observed dependency shows that it will be possible to minimize C incorporation by supplying enough reactive H or MO rest groups to bond to the C reactive species on the surface before this species bonds to the reactive N species and is incorporated accordingly.

To further clarify whether the C containing species is originating from the N MO source, UDMHy and its temperature-dependent decomposition characteristics, the C content in Ga(NAs) films has been determined in dependence on the growth temperature between 350 and 525 °C, always keeping the N content in the layers at a constant value. This study can be—for simplicity—done for In-free films, as we already

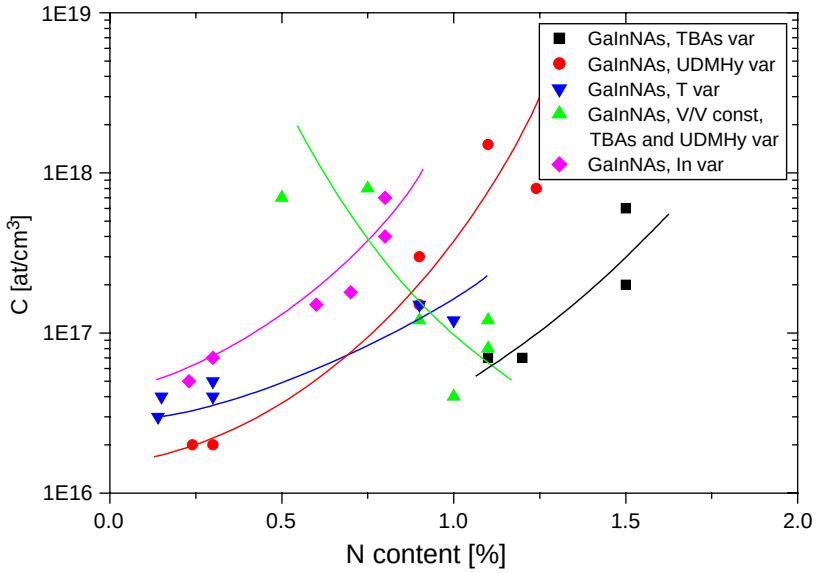

Fig. 4. SIMS carbon content in (GaIn)(NAs) quantum wells in dependence of the N content in the QW for different growth conditions.

excluded TMIn to be the source of C. UDMHy decomposes by breakage of the N–N bond [22] and is still not fully decomposed at the temperatures used. The NH_2 part of the molecule is consumed for N incorporation, while the dimethylamine radical should not be incorporated, it however might also decompose in what results as the formation of CH_3 radicals [22], which could certainly be a source of C. The decomposition of the dimethylamine radical starts only at temperatures above 500 °C. Hence, we should observe a strong decrease of the C content with dropping growth temperature if the UDMHy would be the source of the C.

To further clarify this, we also measured the C content in GaAs grown under the same conditions using another N source, TBHy, to perform the same experiments. TBHy is completely decomposed in the temperature range under investigation [23] and no C incorporation at all should be expected from this molecule. The C content in GaAs (circles) and Ga(NAs) from UDMHy (open squares) and TBHy (filled squares) is plotted in dependence of the growth temperature in Fig. 5. The C incorporation already shows a significant

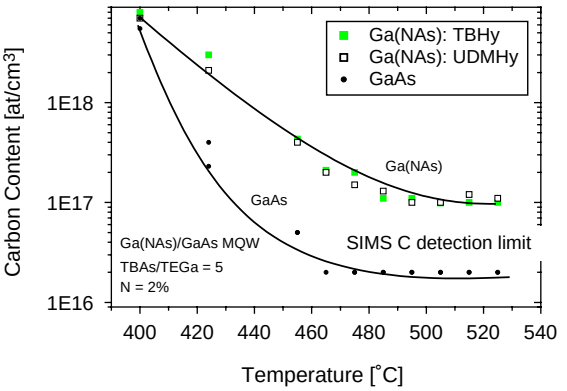

Fig. 5. SIMS carbon content in Ga(NAs) quantum wells and GaAs barriers for different growth temperatures using UDMHy as well as TBHy as N sources.

dependence on temperature for pure GaAs growth with no N source in the reactor. This C incorporation can only be attributed to the TEGa, as the TBAs as C source has been excluded (Fig. 4). Carbon from the ethyl group of the TEGa could be incorporated if the β hydride elimination of ethane, via which TEGa is

decomposing is not effective at the low growth temperatures. C incorporation into Ga(NAs) is higher than in GaAs, but identical for both N sources UDMHy and TBHy for the same N content. This indicates that neither of the N precursors is the primary source for C incorporation in the layers. The increased C content we observe, in N containing material is a consequence of the strong C–N bond, which results in the bonding of the ethyl radical (or its decomposition products) to the active N species. Due to this bond strength the C–N containing radical will be incorporated in the growing film. This C incorporation can only be suppressed when supplying enough other radicals to the growth surface so that the active N radical is hindered from bonding to C containing groups at the wafer surface. Hence, further experiments with a constant V/V ratio and increasing partial pressures of both group-V sources have to be undertaken in order to bring the residual C level below $1 \times 10^{16}\,\mathrm{cm}^{-3}$.

The fact that also MBE-grown lasers exhibit high threshold current densities and also in these data a considerable scatter is found in the literature, suggests that the C incorporation in (GaIn)(NAs) is a challenge that is posed for both the growth techniques. Its reduction enables growth of devices that show a better threshold current density and presumably also improved high temperature and lifetime characteristics.

4. Summary

(GaIn)(NAs) is successfully grown by MOVPE to have compositions suitable for both, solar cell and laser applications. In the quaternary metastable material large columnar strain fields have been observed on a lateral length scale of 10–20 nm. These strain fluctuations might be attributed to chain-like ordering of N in as-grown material, which can be dissolved upon annealing, also resulting in improved optoelectronic device characteristics. Furthermore, we found a striking dependence of the threshold current density of (GaIn)(NAs) edge-emitting broad area lasers on the C incorporated in the active material of these lasers. The C is incorporated together with N due to the strength of the C–N bond. Detailed growth studies applying different N precursors (UDMHY, TBHy) with varying V/V- and V/III-ratios and growth temperature point to TEGa as the source of C-containing radicals, leading to increased C uptake at low deposition temperatures. However, C incorporation can be minimized by using appropriate V/V and V/III ratios leading to improved device characteristics.

Acknowledgement

Various parts of this work have been supported by the Deutsche Forschungsgemeinschaft in the framework of the Forschergruppe "Metastable Compound Semiconductors and Heterostructures", the Federal Ministry of Education and Research (BMBF) as well as by Akzo Nobel, HPMO.

References

[1] M. Kondow, K. Uomi, A. Niwa, T. Kitatani, S. Watahiki, Y. Yazawa, Jpn. J. Appl. Phys. 35 (1996) 1273.
[2] S.H. Wei, A. Zunger, Phys. Rev. Lett. 76 (1996) 664.
[3] L. Bellaiche, Appl. Phys. Lett. 75 (1999) 2578.
[4] S.R. Kurtz, D. Myers, J.M. Olson, in: 26th IEEE Photovoltaic Specialists Conference, IEEE, New York, Anaheim, 1997, pp. 875.
[5] D.J. Friedman, J.F. Geisz, S.R. Kurtz, J.M. Olson, J. Crystal Growth 195 (1998) 409.
[6] S.R. Kurtz, A.A. Allerman, E.D. Jones, J.M. Gee, J.J. Banas, B.E. Hammons, Appl. Phys. Lett. 74 (5) (1999) 729.
[7] C. Baur, A. W. Bett, F. Dimroth, S. V. Riesen, B. Kunert, M. Traversa, K. Volz, W. Stolz, Proceedings of the WCPEC-3, Osaka, Japan, 2003, pp. 677.
[8] N. Tansu, J-Y. Yeh, L.J. Mawst, Appl. Phys. Lett. 83 (13) (2003) 2512.
[9] F. Höhnsdorf, J. Koch, S. Leu, W. Stolz, B. Borchert, M. Druminski, Electron. Lett. 35 (1999) 571.
[10] S. Bank, W. Ha, V. Gambin, M. Wistey, H. Yuen, L. Goddard, S. Kim, J.S. Harris, J. Crystal Growth 251 (1–4) (2003) 367.
[11] K. Volz, J. Koch, B. Kunert, W. Stolz, J. Crystal Growth 248 (2003) 451–456.
[12] K. Volz, T. Torunski, W. Stolz, J. Appl. Phys., in press.
[13] P.N. Keating, Phys. Rev. 145 (1966) 637.
[14] R.M. Martin, Phys. Rev. B 1 (1970) 4005.
[15] P.R.C. Kent, A. Zunger, Phys. Rev. B 64 (2001) 115208.
[16] C. Persson, A. Zunger, Phys. Rev. 68 (2003) 035212.

[17] T. Kitani, M. Kondow, T. Tanaka, J. Crystal Growth 227–228 (2001) 521.
[18] P.J. Klar, H. Grüning, J. Koch, S. Schäfer, K. Volz, W. Stolz, W. Heimbrodt, A.M.K. Saadi, A. Lindsay, E.P. O'Reilly, Phys. Rev. B 64 (2003) 161201.
[19] S. Kurtz, J. Webb, L. Gedvilas, D. Friedman, J. Geisz, J. Olson, R. King, D. Joslin, N. Karam, Appl. Phys. Lett. 78 (2001) 748.
[20] M.A. Pinault, E. Tournie, Appl. Phys. Lett. 78 (2001) 1562.
[21] K. Volz, J. Koch, B. Kunert, W. Stolz, to be published.
[22] E. Bourret-Courchesne, Q. Ye, D.W. Peters, J. Arnold, M. Ahmed, S.J.C. Irvine, R. Kanjolia, L.M. Smith, S.A. Rushworth, J. Crystal Growth 217 (2000) 47.
[23] U.W. Pohl, C. Möller, K. Knorr, W. Richter, J. Gottfriedsen, H. Schumann, K. Rademann, A. Fielicke, Mar. Sci. Eng. B 59 (1999) 20.